

Silicon-on-Insulator Nanowire Based Optical Waveguide Biosensors

Mingyu Li, Yong Liu, Yangqing Chen and Jian-Jun He

State Key Laboratory of Modern Optical Instrumentation, Zhejiang University, Hangzhou, China, 310027

jjhe@zju.edu.cn

Abstract. Optical waveguide biosensors based on silicon-on-insulator (SOI) nanowire have been developed for label free molecular detection. This paper reviews our work on the design, fabrication and measurement of SOI nanowire based high-sensitivity biosensors employing Vernier effect. Biosensing experiments using cascaded double-ring sensor and Mach-Zehndering sensor integrated with microfluidic channels are demonstrated

1. Introduction

Optical waveguide sensors based on silicon-on-insulator (SOI) nanowire have received great attention due to their potential applications in many fields including bacteria and virus detection, medical diagnostics, food quality control, environment monitoring, drug development and so on. Various types of SOI sensors have been developed, including Mach-Zehnder interferometer [1], microdisks [2] and microring resonators [3]. Among various types of optical waveguide sensors, microring resonators have been regarded as a promising solution for biological recognition and chemical analysis.

Optical waveguide biosensor is the device which can give the measurable signal when the target molecule is bond to another biomolecule on the surface of waveguide. Intensity interrogation and wavelength interrogation are two typical sensing methods for SOI nanowire based optical waveguide sensor. Both of these methods require a high resolution spectrometer or a narrow line-width tunable laser to achieve a high sensitivity. These instruments are very expensive and cannot be integrated on chip. To solve these problems, cascaded double microring resonators and a Mach-Zehnder interferometer (MZI) cascaded with a microring resonator employing Vernier effect were proposed [4,5]. Label-free detection capability of these two types of SOI sensors have also been demonstrated.

2. Cascaded double-ring sensor

The double-ring sensor consists of a sensing ring and a reference ring cascaded by a bus waveguide as shown in Fig.1. The whole chip was covered by Su8 upper cladding layer except that the sensing ring is exposed to the analyte sample by removing the upper cladding layer in the sensing window. The two rings have slightly different perimeter length and thus different free spectral ranges (FSRs) to produce a Vernier effect. Compared to a single microring resonator, the peak wavelength shift in the envelope function of the transmission of the cascaded double ring resonators is magnified by a Vernier amplification factor

$$F = \frac{\Delta\lambda_{FSRr}}{|\Delta\lambda_{FSRr} - \Delta\lambda_{FSRs}|} \quad (1)$$



where $\Delta\lambda_{FSRr}$ and $\Delta\lambda_{FSRs}$ are the FSR of the reference ring and sensing ring, respectively.



Fig. 1 Optical microscope image of the cascaded double ring sensor based on SOI nanowire.

The sensor is designed on SOI substrate with a 220 nm Si layer on a 2 μm SiO₂ layer. Since SOI is a high refractive index contrast material, the waveguide should be designed to be very small to keep the single mode of the waveguide. In our design, the widths of all the ridge waveguides are designed to be 1 μm with a shallow etched ridge height of 50 nm in order to maintain the single mode. We choose directional coupler to couple light into and out of the micro-ring resonators with the minimal distance between the bus waveguide and ring to be 1 μm , so that the optical sensor can be fabricated by contact photolithography.

The FSRs of reference ring and sensing ring are 0.7487nm and 0.6774nm, corresponding to $F=10$. Figure 2 shows the measured transmission spectra when sensing ring is exposed to solution of NaCl with different concentration of 2%,4%,6% and 8%. When the sample was changed, the sensing window was rinsed by the next new measuring solution. Figure 3 shows the measured central wavelength shift as a function of refractive index change of solution sample. The wavelength shift sensitivity is about 220nm/RIU. The detection limit using central peak wavelength shift detection is 3.3×10^{-3} RIU.

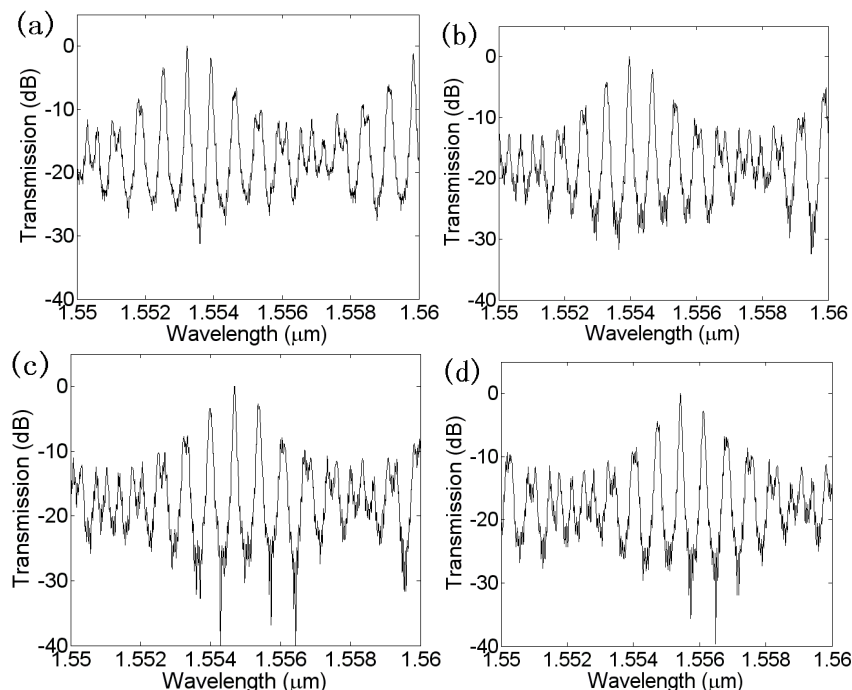


Fig.2 Measured transmission spectra of the cascaded double ring with different concentrations of NaCl solutions of 2%(a), 4%(b),6%(c) and 8%(d).

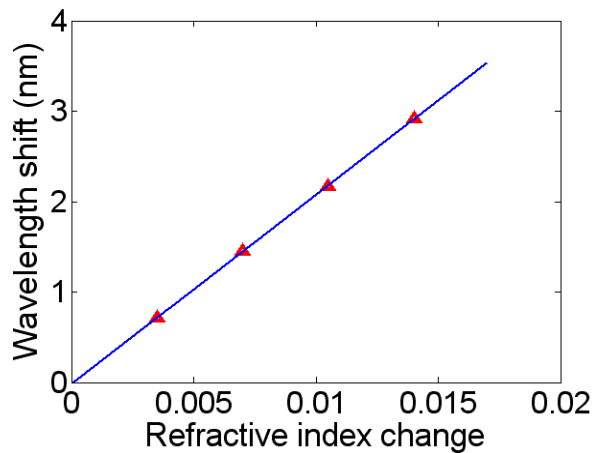


Fig. 3 Measured resonance wavelength shift of the cascaded double ring versus refractive index change of NaCl solutions

For the wavelength interrogation, the peak wavelength shift in the envelope function of the transmission of the cascaded double ring resonators is measured using an optical spectrum analyzer. Since the resonant wavelength of the reference ring is fixed, if one simply looks for the resonant peak of the maximum intensity, the minimal detectable wavelength shift $\delta\lambda_{\min}$ is $\Delta\lambda_{\text{FSRr}}$, corresponding to a wavelength shift of the sensing ring of $\delta\lambda_s = |\Delta\lambda_{\text{FSRr}} - \Delta\lambda_{\text{FSRs}}|$. In order to have a lower detection limit, we made a thoroughly analysis of the transmission spectrum of the cascaded double ring, finding that the intensity ratio of the two central peaks varies with the refractive index change of the analyte. Experimentally, we proved that the detection limit can be dramatically improved by combining the detection of the intensity ratio between two central peaks [4]. In order to demonstrate this method, we used the solutions of NaCl with smaller concentration variations. Figure 4 shows the measured transmission spectra of the sensor when sensing ring is exposed to solutions of NaCl with different concentrations of 0.4%, 0.8%, 1.2% and 1.6%, respectively.

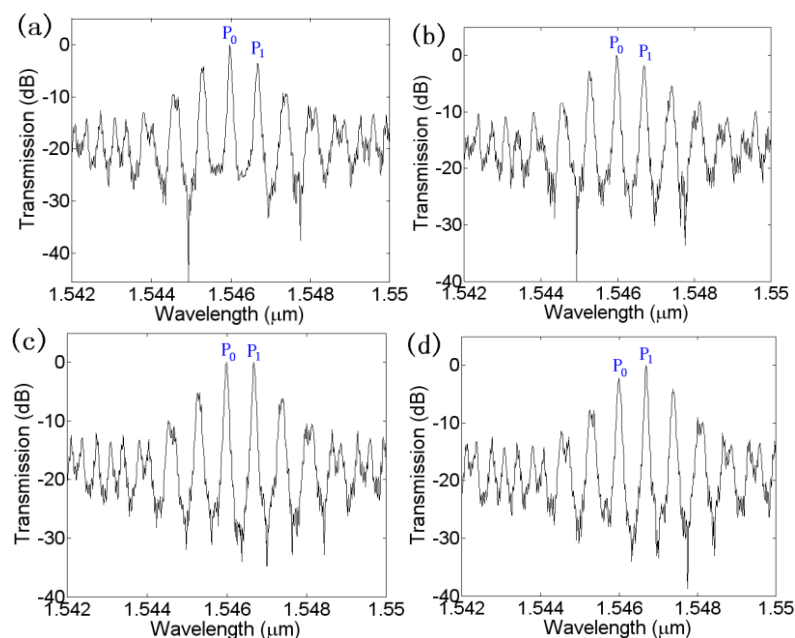


Fig. 4 Measured transmission spectra of the cascaded double ring with different concentrations of NaCl solutions of 0.4%(a), 0.8%(b), 1.2%(c) and 1.6%(d)

The measured intensity ratio between the two central peaks, as a function of refractive index change of solution is shown in figure 5. The sensitivity is 2500 dB/RIU. The detection limit is 4×10^{-6} RIU.

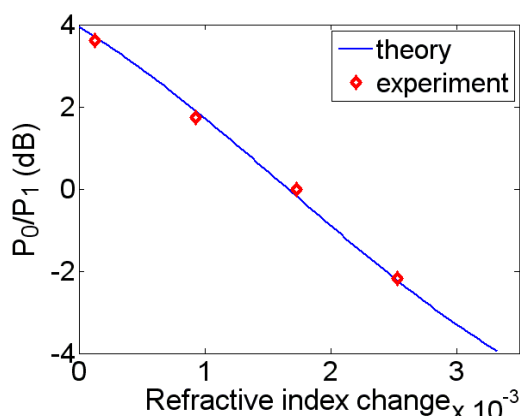


Fig.5 Measured intensities ratio P_0/P_1 of the two central peaks versus the refractive index change of NaCl solutions.

To reduce the cost of measurement system, the sensor can be operated in intensity interrogation using low cost broadband source without requiring wavelength information [6]. When a broadband light source such as an LED is used, the output power will change in proportion to the overlap integral of the LED spectrum and envelope function of the transmission spectrum. Assume the central wavelength of LED coincide with the peak of wavelength of the transmission envelop function initially. When n changes, the peak wavelength of the transmission shifts and they have a relative displacement. Consequently, the total output spectrum changes. Therefore, we can detect the variation of the sample refractive index by measuring the change of the total power. In this experiment, the difference of the FSRs for the two rings is 0.67%, which corresponds to an amplification factor $M=150$

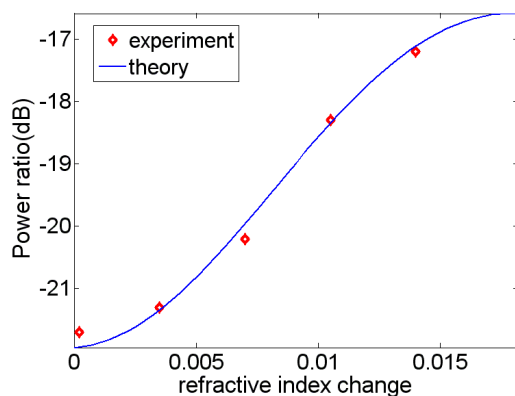


Fig.6 Power ratio between signal port and reference port vs. Refractive index change

Figure 6 shows the normalized output power versus the sample refractive index change of salt solution. By fitting the measured data with theoretical calculation, the sensitivity of the sensor reaches about 450 dB/RIU without requiring the spectral measurement. However, the detection limit of intensity interrogation is larger than that of the wavelength interrogation.

By using the standard silicon surface functionalization procedure, the anti-human IgG is immobilized on the surface of the sensing area of the sensor chip. The figure 7 shows the calibration curves for hIgG determination. From the transmission responses of the cascaded double ring exposed to solutions with different concentrations of hIgG, the concentration of 7.1–125 $\mu\text{g/mL}$ was measured in the linear detection range [7]. The detection limit down to 7.1 $\mu\text{g/ml}$ with 0.47nm wavelength resolution. As a contrast, we also tested the chip with solution of casein and found no wavelength shift, which proves the specific recognition of the anti-hIgG functionalized surface for hIgG. The cascaded double ring sensors can be implemented in an array for potential simultaneous detection of multiple species.

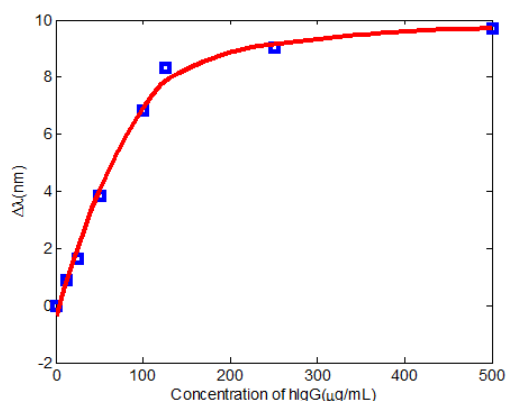


Fig.7 The wavelength shift of the transmission curve Calibration curves for hIgG determination

3. Cascaded MZI-ring sensor

Recently, an ultrahigh-sensitivity SOI nanowire optical waveguide biosensor based on cascaded MZI and ring resonator with Vernier effect using wavelength interrogation is proposed and experimentally demonstrated [5]. Fig. 8 shows the optical microscope image of the sensor. The sensor consists of a MZI cascaded with a ring resonator, in which, the MZI is used for sensing while the ring resonator acts as a reference. Using the cascaded MZI-ring, the wavelength shift of the MZI is translated into a much larger shift of the total transmission envelope function due to the Vernier effect. It's very similar to the cascaded double ring sensor. For a cascaded double ring resonator sensor, the Δ FSR of the sensing ring and reference ring has to be designed fairly small to get a large F. while a small Δ FSR means a flat envelope function of the total transmission spectrum, making it hard to determine the wavelength shift accurately. However, for the novel MZI-ring sensor, the Δ FSR of the MZI and the ring resonator can be designed relatively larger while still maintain almost a same level of sensitivity.

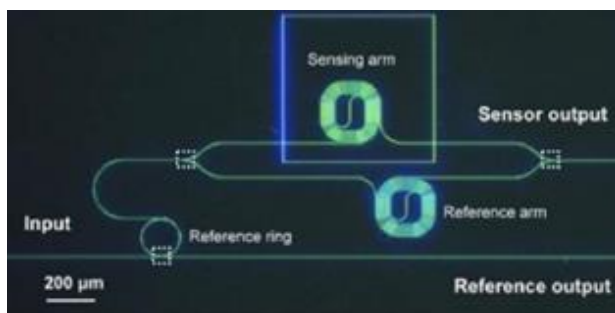


Fig.8 Optical microscope image of the cascaded MZI- ring sensor

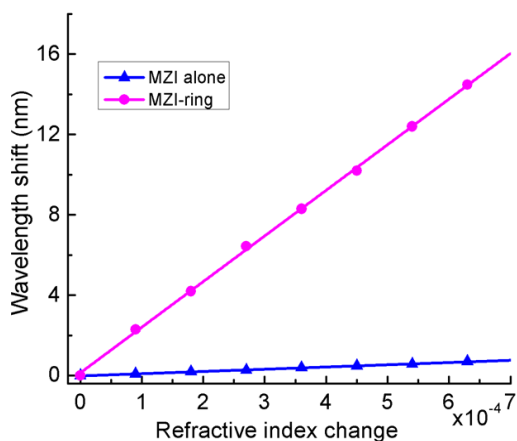


Fig. 9 Measured wavelength shift versus refractive index change of NaCl solutions with different concentrations

According to the wavelength peak shift in the measured transmission spectra of MZI-ring sensor with NaCl solution of different concentrations, the sensitivities for MZI sensor and cascaded MZI-ring sensor are 370nm/RIU and 19100nm/RIU respectively as shown in figure 9.

The wavelength shift of the MZI-ring sensor is about 14 times larger than that of the MZI sensor alone. To investigate the temperature dependence of the sensors, TEC was used to heat the sensor, the wavelength shifts versus temperature change are shown in figure 10. The measured results indicate that MZI-ring sensor is sensitive to the temperature, so using thermoelectric cooler (TEC) control the temperature is necessary in extremely low concentration detection.

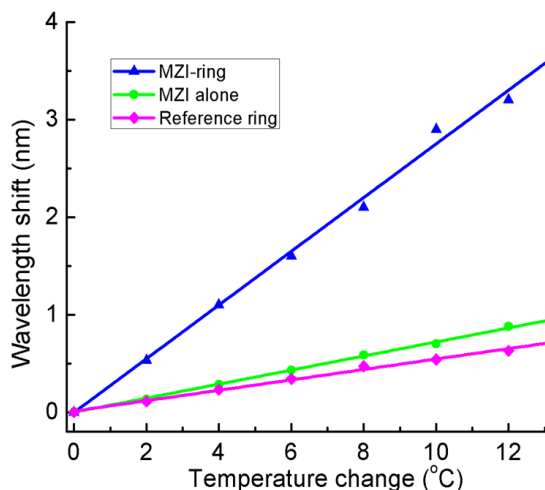


Fig. 10 Wavelength shift versus temperature change for reference ring, MZI and MZI-ring

After the standard surface functionalization on the sensing arm of the MZI, the sensor was used for monitoring the binding reactions between goat and antigoat IgG pairs. TEC maintained the sensor at 25°C during the measurement. The measured sensor response is shown in the figure 11.

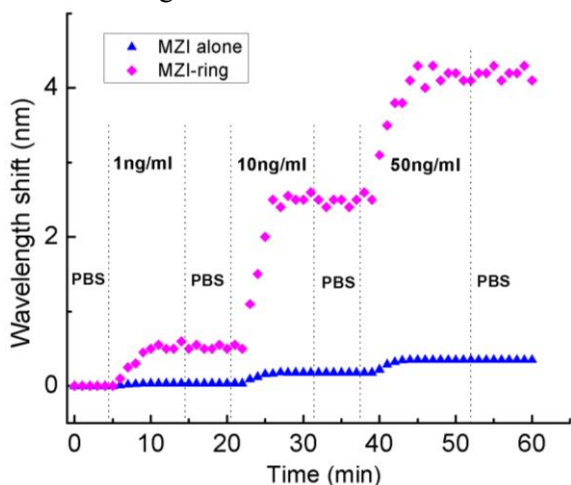


Fig. 11 Wavelength shift of the sensors with injection of antigoat IgG with different concentrations.

While the wavelength shift of the MZI-ring sensor is about 14 times larger than that of the MZI sensor, the wavelength measurement error also increased due to the peak broadening in the envelope function. The estimated lowest detectable concentration for the MZI sensor is about 0.29 ng/ml IgG with a minimal detectable wavelength shift of 10 pm. For the MZI-ring sensor, the reliable minimal detectable wavelength shift is around 50 pm using data fitting, which gives the lowest detectable concentration of 0.1 ng/ml IgG.

Although, the requirement of the spectral resolution is 5 times lower, the sensitivity of the MZI-ring is still about 3 times higher than that of MZI sensor. Thus, the sensor can detect extremely low concentration of IgG.

4. Conclusion

Cascaded double-ring sensor and MZI-ring sensor employing the Vernier effect have been proposed and experimentally demonstrated. The experimental results show that Vernier effect can increase the sensitivity dramatically. These SOI nanowire based high-sensitivity optical waveguide sensors are promising for real time measurements of molecule binding kinetics in biomedical and chemical applications.

Acknowledgment

This work was supported by the National High-Tech Research and Development Program of China (No. 2014AA06A504), the Science and Technology Department of Zhejiang Province (No. 2014C31030), Fundamental Research Funds for Central Universities (No. 2014QNA5018), and the National Natural Science Foundation of China (No. 61535010), Zhejiang Provincial Natural Science Foundation of China (No. LY16F050001).

References

- [1] B. Sepulveda, J.S. Del Rio, M. Moreno, F. Blanco, K. Mayora, C. Domínguez, L.M. Lechuga, "Optical biosensor microsystems based on the integration of highly sensitive Mach–Zehnder interferometer devices", *Opt. A: Pure Appl. Opt.*, 8 S561-S566 (2006)..
- [2] R.W. Boyd, J.E. Heebner, Sensitive disk resonator photonic biosensor, *Appl. Opt.*, 40(31), 5742-5747 (2001)
- [3] J.T. Kindt, R.C. Bailey, "Biomolecular analysis with microring resonators: Applications in multiplexed diagnostics and interaction screening", *Curr. Opin.Chem.Biol.*, 17,818-826 (2013).
- [4] L. Jin, M. Li, J.-J. He, "Highly-sensitive silicon-on-insulator sensor based on two cascaded micro-ring resonators with vernier effect", *Opt. Commun.*, 284 (2011) 156-159.
- [5] X. Jiang, Y. Chen, F. Yu, T. Tang, M. Li, J.-J. He, "High-sensitivity optical biosensor based on cascaded Mach-Zehnder interferometer and ring resonator using Vernier effect", *Opt. Lett.*, 39(15), 6363-6365 (2014).
- [6] L. Jin, M. Li, and J.-J. He, "Optical waveguide double-ring sensor using intensity interrogation with low-cost broadband source", *Opt. Lett.* 36(7), 1128–1130 (2011).
- [7] Y. Chen, F. Yu, C. Yang, J. Song, L. Tang, M. Li, J.-J. He, "Label-free biosensing using cascaded double-microring resonators integrated with microfluidic channels", *Opt. Commun.* 344, 129-133 (2015).